Research Papers
Issue RP0136
July 2012

ISC - Impacts on Soil and Coasts Division

Prearrangement of the COSMO-CLM Model on the Chinese region and sensitivity analysis

By **Edoardo Bucchignani**
Centro Italiano Ricerche Aerospaziali, CIRA
Impacts on Soil and Coasts Division, CMCC
e.bucchignani@cira.it

Paola Mercogliano
Centro Italiano Ricerche Aerospaziali, CIRA
Impacts on Soil and Coasts Division, CMCC
p.mercogliano@cira.it

Myriam Montesarchio
Impacts on Soil and Coasts Division, CMCC
m.montesarchio@cira.it

Alessandra Zollo
Impacts on Soil and Coasts Division, CMCC
a.zollo@cira.it

and **Maria Paola Manzi**
Impacts on Soil and Coasts Division, CMCC
m.manzi@cira.it

SUMMARY This report represents the description of the first activity performed within the work package 7.1.6 of the "B action" in the Gemina project. The "B action" of the Gemina project concerns the consolidation and development of international scientific network. In particular the cooperation between China and Italy is focused on the development of regional climate scenarios and the analysis of impacts on coastal areas on the Chinese region. The main goal of the WP 7.1.6. is to provide high resolution climate simulation on the China region for the XXI century. In order to perform this activity, some preliminary simulations are requested, to find an optimal configuration for the high resolution climate model COSMO CLM. This report contains the description of the sensitivity analysis developed on a limited part of the Chinese region.

This report represents the Deliverable P162 developed within the framework of Work Package 7.1.6 Action B of the GEMINA Project, funded by the Italian Ministry of Education, University and Research and the Italian Ministry of Environment, Land and Sea.

INTRODUCTION

As reported in the white paper (White paper: China's policies and actions on climate change,$http://www.china.org.cn/government/news/2008-10/29/content\_16681689\_4.htm$) of the China government, China is one of the countries most susceptible to the adverse effects of climate change, mainly in the fields of agriculture, livestock breeding, forestry, natural ecosystems, water resources, and coastal zones. The detection of climate changes impact is mostly felt at local characteristic of the climate. For these reasons a quantitative evaluation on the risk modifications due to climate change requires a downscaling of the GCM model. In fact these last ones operate at scales too coarse to study systems of interest in impacts and adaptation research, so a downscaling procedure is necessary. Many different statistical downscaling approaches can be found in literature. These statistical approaches have an important limitation: they rely on the existence of a long historical observational record from which statistical relationships can be calculated and used to extrapolate information on the future climate only in the area in which data are available and only for the variables for which time histories are available. An alternative approach could be provided by the Dynamical downscaling, related to the use of Regional Climate Models (RCMs). RCMs have some advantages over statistical techniques: they simulate the entire climate system so that all climate variables of interest are available, rather than being limited to the observed variables; and they simulate the climate regardless the availability of observations. The local analysis, in particular, is a necessary tool in areas with a complex topography, which strongly forces and influences regional and local climate. The area of China, as a consequence of its large dimensions and its complex geography, exhibits a variety of different climates. Global climate models (GCM) are generally unsuitable to simulate climate at local scale, since they are characterized by resolutions generally around or coarser than 100 km. The usage of a Regional Climate Model (RCM) with a horizontal resolution of about 10 km can be a useful tool for the description of the climate variability on local scale.

For all these motivations the CMCC, in particular the ISC division, is involved, in the frame of the CLM Community, ($www.clm-community.eu$) in the development of the RCM COSMO CLM with the goal of describing the local features of the climate. In the last years, the CMCC ISC team has successfully used the regional climate model COSMO-CLM in different projects, simulating the climate of several areas located inside Europe (such as FP7 ENV SafeLand, Interreg Adaptalp) and Africa (such us FP7 ENV CLUVA).

The activity described in this report represents the first attempt of CMCC ISC team to perform climate simulations in Asia, and in particular over China, with COSMO-CLM. For this reason, it was necessary to conduct a preliminary analysis aimed to choose an optimal set up of the model, suitable to reproduce in a realistic way the present climate of the area under study.

The results of this analysis are described in this document, which is organized in the following main sections: description of the motivations of this work; analysis of the main features of the climate of China; detailed description of the activity performed with COSMO-CLM; analysis and discussion of the results obtained with the different configurations tested; main conclusions.

MOTIVATION

Regional Climate Models allow investigating the temporal and spatial evolution of the climate of a limited area, enabling to simulate the climate at higher temporal and spatial resolution and adding significant skill in simulating the climate on a scale from 1 to 50 km. The CCLM [11] is the climate version of the COSMO model [13], the operational non-hydrostatic mesoscale weather forecast model developed at the German Weather Service. Successively, the model has been modified by the CLM-Community, in order to develop also climatic applications. The updates of its dynamical and physical packages allow its application in cloud resolving scales.
The COSMO-CLM model offers the opportunity to use different options for model domain, formulation of model physics and dynamics, by setting the values of the so called NAMELIST Parameters, grouped in NAMELIST blocks of the COSMO model, being more than 150 parameters. Some of the namelist parameters depend clearly on horizontal or vertical resolution, time step and region selected on the globe. Each list of settings is named as a possible Configuration of the COSMO model run.
Previous studies have highlighted that the configuration of a regional model in general cannot be transferred directly to other climatic areas straightforward, but rather making specific modifications requested in each case. Preliminary evaluation of COSMO CLM on different worldwide regions have been performed by Rockel and Geyer [10] showing that the standard set up of COSMO LM, the one used in the Europe region, should only be applied to those regions on the globe which have similar climate charactestichs to Europe's. For other climate zones, especially the tropics, a modified setup is necessary. The COSMO CLM setup requires a quite long simulation activity due to the different physical parameterizations and numerical scheme implemented in the model. The purpose of this study is, therefore, the definition of an optimal configuration in order to make COSMO CLM suitable, mainly in terms of precipitation and 2 meter temperature, to perform climatic simulations over the Chinese area.

CHINA CLIMATE AND CLIMATE CHANGE: GENERAL FEATURES

China is a large country in eastern Asia covering about 3.7 million square miles. The world's highest mountains, the Himalayas, are in China, such us one of the world's largest deserts, the Taklamakan Desert. China also boasts some of the longest rivers in the world. The climate of China is,therefore, extremely different, depending on the region [16]. Differences in latitude, longitude and altitude give rise to sharp variations in precipitation and temperature. Monsoon winds, caused by differences in the heat-absorbing capacity of the continent and the ocean, dominate the climate: the advance and retreat of the monsoons account in large degree for the timing of the rainy season and the amount of rainfall in the country. Alternating seasonal air-mass movements and accompanying winds are moist in summer and dry in winter. Figures 1 and 2 show a subdivision of China in different climatic zones and some features of the different climate zones
($From\ http://chinagtn.org/?q = node/8$).

A tropical climate is in the south, which is characterized by a lush vegetation: during the summer season, there is an average temperature of about 28°C, while in winter these are about 10°C. A colder weather is present in the northern and eastern area. In these areas, the temperatures can also come under -5°C in January, while in summer the average temperature does not usually exceed 20°C.

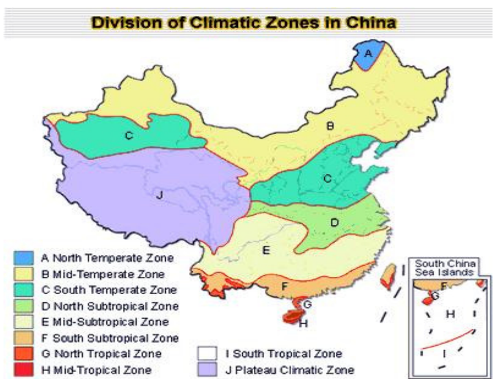

Figure 1:
Subdivision of China in different climatic zones

Map Key	Description
B – Mid–Temperate zone	Zone described as coldest month average temperature –3 C. Average temperature of warmest month above 10C.
C – South–Temperature zone	Coldest month has an average temperature below 18 C but above 10 C. Climate has both a summer and winter
D – North Subtropical zone	Coldest month has an average temperature under 18 C. Precipitation is adequate for all months. Climate has both a summer and winter.
E – Mid–Subtropical zone	Coldest month as an average temperature under 18 C and adequate preciptiation. The warmest month's mean is under 22 C with at least 4 months having means over 10 C
F, G & H – South–Subtropical to North Tropical zone	Monthly mean temperatures over 18 C but in some areas the coldest average temperature slightly under 18 C. Adequate moisture present
J – Plataeu zone	Both dry and cold temperatures with a significant lack of moisture

Figure 2:
Features of the different Chinese climatic zones introduced in the previous figure

The main cities are characterized by the following temperature ranges:

- Beijing: from 4°C to 25-27°C
- Shanghai: from 3-4°C to 28-30°C

Figure 3 shows the mean annual temperature during the period 1961-2003 in China. Precipitation varies regionally even more than temperature. In the south (in particular Qin Mountains area) there is abundant rainfall, often above 1000 mm, most of it coming with the monsoon during summer and late spring. The northwest

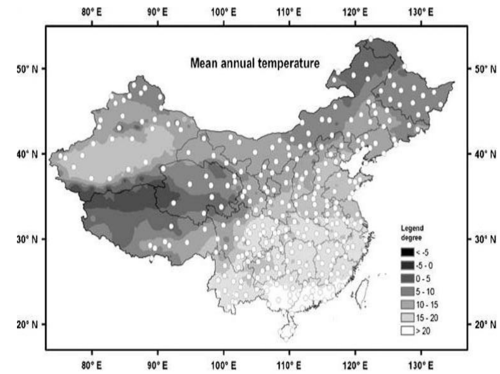

Figure 3:
The mean annual temperature during 1961-2003 in China (from Q.You et al., 2010)

has the lowest annual rainfall with any precipitation in desert areas. China experiences frequent typhoons, damaging floods, tsunami, dust storms and drought. Figure 4 shows the mean annual precipitation during the period 1961-2003 in China.

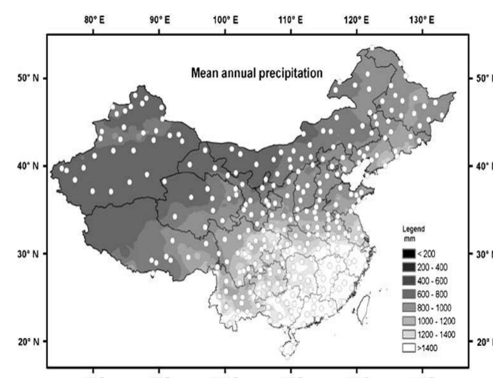

Figure 4:
The mean annual precipitation during 1961-2003 in China (from Q.You et al., 2010)

Over the past several decades, China has already experienced some devastating climate extremes [9]. In particular in Figure 5 it is reported (red dots) the areas with a significant (P,0.05) increase in drought expressed by the Palmer Drought Severity Index (PDSI; the higher the index the less drought) during the period 1960-2005; the green dots indicate the areas where a decrease in drought was observed [2].

Figure 5:
Areas affected by increasing and decreasing of flood risk during 1960-2005 (from A. Dai et al., 2004)

A strong warming of China (about 1.2 °C from 1960) over the past five decades is firmly supported by continuous measurements and the warmest years all occurred during the last decade. Winter warming (0.04°C per year) is about four times the rate of summer warming (0.01°C per year), and thus the temperature seasonal cycle amplitude has decreased by 0.03°C per year . Moreover, northern China is warming faster than southern China([4], [15]). For future projections, IPCC global climate models indicates that warming trend will continue, but uncertainties about its extent and pace are large ([7]). An analysis of rain gauge stations indicates that no significant long-term trend in country-average precipitation since 1960 have been observed. However, there are significant regional precipitation trends. The drier regions of northeastern China (including North China and Northeast China) are receiving less and less precipitation in summer and autumn. By contrast, the wetter region of southern China is experiencing more rainfall during both summer and winter. Similar regional summer precipitation trends are expected from the probable weakening of the summer monsoon since the late 1970 ([3]). So far, the changes appear to fall within the bounds of normal decadal variability of rainfall ([9]). Future projections of precipitation by IPCC climate models are highly uncertain ([7]).

HIGH RESOLUTION CLIMATE SIMULATIONS

COSMO CLM

The regional climate model COSMO-CLM [11] can be used with a spatial resolution between 1 and 50 km even if the non hydrostatic formulation of the dynamical equations in LM made it eligible especially for the use at horizontal grid resolution lesser than 20 km [1]. These values of resolution are usually close to those requested by the impact modellers; in fact these resolutions allow to describe the terrain orography better than the global models, where there is an over- and underestimation of valley and mountain heights, leading to errors in precipitation estimation, as this is closely related to terrain height. Moreover the non-hydrostatic modelling allows providing a good description of the convective phenomena, which are generated by vertical movement (through transport and turbulent mixing) of the properties of the fluid as energy (heat), water vapour and momentum. Convection can redistribute significant amounts of moisture, heat and mass on small temporal and spatial scales. Furthermore convection can cause severe precipitation events (as thunderstorm or cluster of thunderstorms). Another advantage related to the usage of COSMO-CLM, with respect to other climate regional models available, is that the continuous development of LM allows improvements in the code that are also adopted in the climate version, ensuring that the central code is continuously update. The mathematical formulation of COSMO-CLM is made up of the Navier-Stokes equations for a compressible flow [5]. The atmosphere is treated as a multicomponent fluid (made up of dry air, water vapour, liquid and solid water) for which the perfect gas equation holds, and subject to the gravity and to the Coriolis forces. The model includes several parameterizations, in order to keep into account, at least in a statistical manner, several phenomena that take place on unresolved scales, but that have significant effects on the meteorological interest scales (for example, interaction with the orography). The main features of the COSMO-CLM are:

- Nonhydrostatic, full compressible hydro-thermodynamical equations in advection form.
- The base state is hydrostatic, at rest.
- The prognostic variables are: horizontal and vertical Cartesian wind components, pressure perturbation, temperature, specific humidity, cloud water content. Optionally: cloud ice content, turbulent kinetic energy, specific water content of rain, snow and graupel.
- The coordinate system is a generalized terrain-following height coordinate with rotated geographical coordinates and user defined grid stretching in the vertical. Options for (i) base-state pressure based height coordinate, (ii) Gal-Chen height coordinate and (iii) exponential height coordinate (SLEVE) according to [12].
- The grid structure is an Arakawa C-grid with Lorenz vertical grid staggering.
- The time integration is based on a time splitting between fast and slow modes (Leapfrog, Runge-Kutta).
- The Spatial discretization is performed with a second order accurate Finite Difference technique.
- The parallelization is based on a Domain Decomposition (MPI as message passing S/W).
- The Parameterizations available are: Subgrid-Scale Turbulence, Surface Layer Parameterization, Grid-Scale Clouds and Precipitation, Subgrid-Scale Clouds, Moist Convection, Shallow Convection, Radiation, Soil Model, Terrain and Surface Data.

The versions used of INT2LM and COSMO-CLM are respectively: int2lm_091216_1.10_clm2 and cosmo_090213_4.8_clm13. In the COSMO Model, it is implemented the soil model `TERRA_ML` which includes melting processes, while the convection scheme used is the Tiedtke one.

THE AREA OF INTEREST

In the present work, a sensitivity analysis to different parameters, in particular physical parameterization and numerical scheme, have been performed over the domain (111 -123 E; 29 - 41.5 N), which has an extension of about 1350 x 1400 km. This domain, shown in Fig. 6, is located in the north-west area of China. A spatial resolution of 0.0715° (about 8 km) has been employed.

The time period investigated by these numerical simulations is 1996-2000. In order to neglect the initial spin up effects the period considered for the model performances evaluation

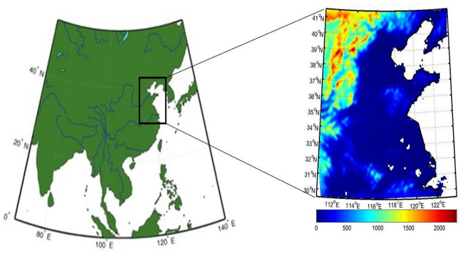

Figure 6:
The domain under study: its location inside China (left) and its orography (right)

is 1997-2000,
The main aimo of the present sensitivity analysis is to find the best COSMO CLM configuration on the Chinese area. In order to neglect the error due the usage of global models, the ERA40 Reanalysis [14] have been used as forcing data. ERA40 dataset is characterized by 320 x 160 grid points, 49 atmospherical vertical level and 3 levels of soil. The resolution of the ERA40 data is 1.125° (about 128 km).
The domain analyzed is discretized with a grid of 170x175 points, with 40 atmospherical vertical levels and 4 soil levels plus a climatological layer (the depth of the different soil levels are 0.03, 0.19, 0.78, 2.28 and 6.98 m). The boundary conditions are updated every 6 hours, while the results are saved every 3 hours. The results have been compared with the CRU data [8]: it is a dataset with monthly observed data of 2-metre temperature and total precipitation amount for the period 1901-2006, at a resolution of 0.5° (about 60 km).

THE REFERENCE NAMELIST

As already explained, in this work we have considered as reference configuration for INT2LM and COSMO the one used for the previous analysis concerning different domains in the Mediterranean area. This configuration represents the starting point of the activity; the simulation performed with this configuration is named as **Run 1**. Then, other configurations have been obtained starting from the last one, by varying one or more key parameteres, in order to analyze the response of the model to these changes.
In the following, a general description of the parameters representing the most important settings and parameterizations of the physics and dynamics of the reference configuration is given.

INT2LM configuration

In this configuration, the sub-grid scale orography scheme used [6] deals explicitly with a low-level flow, which is blocked when the sub-grid scale orography is sufficiently high. For this blocked flow, a separation occurs at the mountain flanks, resulting in a form drag.
A multi-layer soil level has been used.
Finally, a pressure based vertical coordinate on input (hybrid sigma-pressure co-ordinate) is used.

COSMO configuration

In the COSMO model reference configuration, a 2 time-level Runge-Kutta time-split scheme is used, with a third order horizontal advection scheme.
A domain mask is used to reduce the standard coefficient for numerical diffusion for u,v and w, temperature and pressure and humidity and cloud water smoothing.
Concerning the physics, a grid-scale precipitation scheme is adopted, with a Kessler-type warm parameterization scheme without ice-phase processes. Cloud cover, water content and ice content are calculated by the default diagnostic scheme.
Concerning the specific vertical turbulent diffusion parameterization, a prognostic TKE-based scheme, including effects from subgrid-scale

condensation/evaporation is used.
The surface-atmosphere transfer is based on diagnostic TKE in the surface layer.
Subgrid-scale processes are included: the model is run with a moist convection parameterization, which computes the effect of moist convection on temperature, water vapour and horizontal wind in the atmosphere, and the precipitations rates of rain and snow at the ground.
Soil processes are included by running the multi-layer soil model TERRA_LM, which includes melting processes within the soil.
A BATS version is used,for the evaporation of bare soil and the transpiration by vegetation.

DESCRIPTION OF THE CONFIGURATIONS TESTED

As explained before, several configurations have been tested, in order to highlight their advantages and disadvantages in well reproducing the climate of the area considered. In the following, the configurations tested are described. More specifically, the main parameters that differ from the basic configurations have been highlighted. Each configuration is identified as **Run-n**, where n varies from 2 to 8.

Run2
For this configuration, the INT2LM namelist has not been modified. In the COSMO namelist have been used a diagnostic initialization of rain and snow and parameterizations for the description of the forest dynamics; moreover the variables for the rapresentation of the clouds have been modified.

Run3
For this configuration, the INT2LM namelist has not been modified. The only difference in the COSMO namelist is that the time step has been halved with respect to the reference configuration.

Run4
For this configuration, the INT2LM namelist has not been modified. In the COSMO namelist, in addition to the modifications inserted in **Run2**, some parameters for setting the turbulent diffusion parameterization has been changed.

Run5
In addition to the variations inserted in **Run4**, the filtering of the real orography has been modified.

Run6
In addition to the variations inserted in **Run5**, the parameter for reducing the standard coefficient for numerical diffusion (in case of humidity and cloud water smoothing) has been modified.

Run7
This simulation uses the same set up for INT2LM and LM, but with an higher numbers of atmospherical and soil levels (with respect to the reference configuration) has been used.

Run8
The configuration is based on the COSMO CLM configuration used for COSMO CLM in the CORDEX project (for details on the project see $http://wcrp.ipsl.jussieu.fr/SF\_RCD\_CORDEX.html$).

ANALYSIS OF THE RESULTS

The results obtained with the eight configurations considered have been analyzed and compared with CRU observation dataset.

Fig.7 shows the 2-metre temperature distribution, averaged over the period 1997-2000, obtained with the reference configuration (Run1). It is clearly evident that the temperature is connected with orography pattern. In summer season, it is lower on the Yellow sea (compared with the winter period), while in the other parts of the domain, it is higher in the summer period.

Fig.8 shows the daily total precipitation distribution, averaged over the period 1997-2000, obtained for the reference configuration (Run1): there is not a clear connection with the orography; during the summer, the precipitation are higher than in winter period in the almost part of the domain. The precipitation climatology of the area is well represented if compared with the paper [16] (in this paper, data from about 330 station are analyzed.

Fig. 9 shows the seasonal cycle of 2-metre temperature obtained with the different configurations and with CRU data, over the time period 1997-2000. The figure shows that the temperature seasonal cycle is well captured by all the configurations.

Fig 10 shows the seasonal cycle of the differences between the 2-metre temperature (obtained with every configuration) and the CRU data. From the analysis of this figure, it is evident that COSMO - CLM exhibits a warm bias for all the different configurations. The positive bias is always less then 1.8°C. The Run7 exibits the highest positive bias for all the months (it follows Run3 and Run8); the other configurations have a similar bias.

Fig. 11 shows the seasonal cycle of precipitation obtained with the different configurations and with CRU data, over the time period 1997-2000. The precipitation seasonal cycle is quite well captured by all the configurations, especially in the drier period (from September to March).

Fig 12 shows the seasonal cycle of the differences between the precipitation (obtained with every configuration) and the CRU data. There are some differences among the simulations. Run7 is characterized, in each month, by the lowest precipitation amount. For this reason it has the best performances in the months where there is a positive bias (such as April and June) but the worst for the period with a negative bias (such as December and January). Conversely, the Run3 and Run 8 are characterized by higher values of precipitations; therefore they have the best performances in the months where the other runs exhibit a negative bias but the worst for the period when the other runs are characterized by a positive bias. All the other runs have very similar behaviour; the bias is almost restrained between ± 20 % with the exception of April, June and December. For these months there are no appreciable differences for Run1, Run2, Run4, Run5 and Run6.

Fig 13 shows, with reference to the mean annual temperature, the difference between the results obtained with configuration Run1 and the observed data, respectively for the whole year (left panel), winter (upper right panel) and summer (lower right panel).In winter, a better agreement is registered, being a bias between 1 and -1 degrees for almost part of domain. In summer, it is observed an overestimation in the central area of the domain, with a bias between 2 and 3 degrees.

Fig 14 shows, with reference to the mean annual precipitation, the difference between the results obtained with configuration Run1 and the observed data, respectively for the whole year (left panel), winter (upper right panel) and summer (lower right panel).In winter, a general underestimation is registered in the south of the domain; in summer, a general overestimation is observed in the mountain area (west part of the domain).

In the same way, Figs. 15,17,19,21,23,25 and 27 show, with reference to the mean annual temperature, the difference between the results obtained with the other configurations (Run2... Run8) and the observed data.

In any case, the temperature bias is always limited into the interval ± 2.5 °C. The period JJA has, for each configuration, the highest bias (especially in the central part of the domain) while the period DJF is characterized by a general low error between ± 1 °C.

And finally, Figs. 16, 18 ,20 ,22, 24, 26 and 28 show, with reference to the mean annual precipitation, the difference between the results obtained with the other configurations (Run2... Run8) and the observed data. In the period JJA there is a general overestimation of the rainfall amount in the mountain areas (left part of the domain) up to 50 % otherwise there is a good agreement between observations and model. In DJF there is a general undestimation in particular in the southern part of the domain with flat areas whereas in the coastal norther part there is a general overestimation.

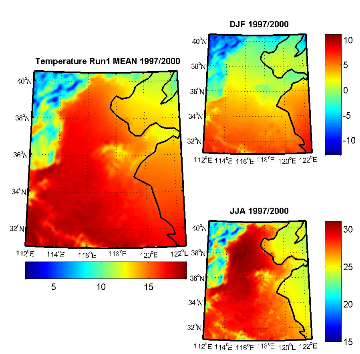

Figure 7:
Distribution of 2-metre temperature, averaged over the period 1997-2000, obtained with configuration Run1

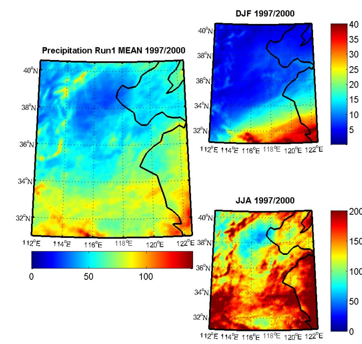

Figure 8:
Distribution of daily total precipitation over the period 1997-2000, obtained with configuration Run1

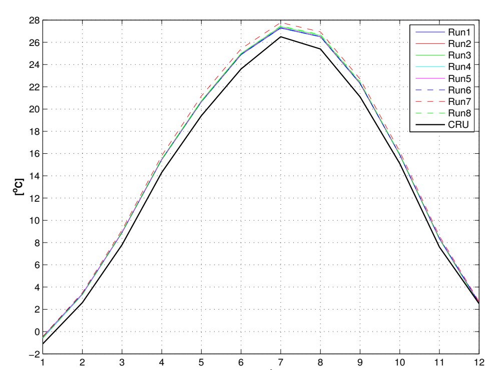

Figure 9:
Seasonal cycle of 2-metre temperature obtained with the different configurations and with CRU data, over the time period 1997-2000.

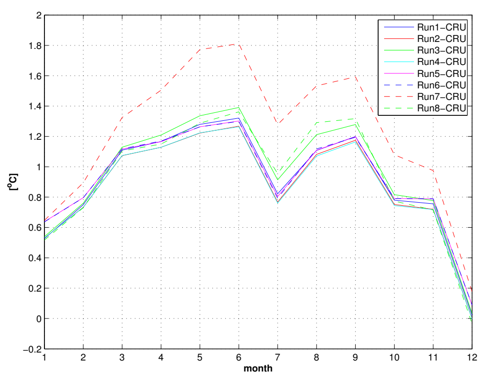

Figure 10:
Seasonal cycle of the differences between the temperature by COSMO-CLM and the observed data for the several cases

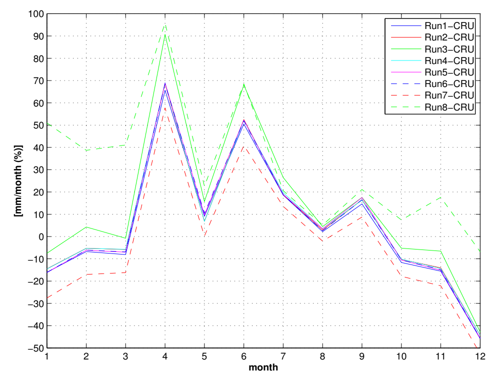

Figure 12:
Seasonal cycle of the differences between the precipitation by COSMO-CLM and the observed data for the several cases

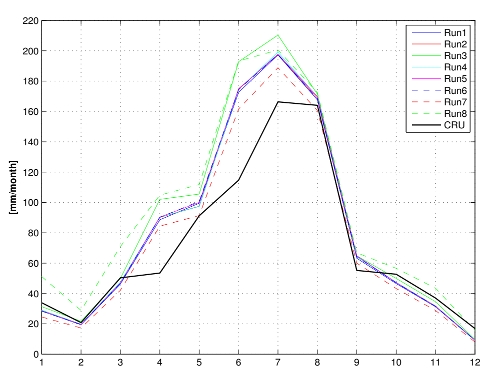

Figure 11:
Seasonal cycle of total precipitation obtained with the different configurations and with CRU data, over the time period 1997-2000.

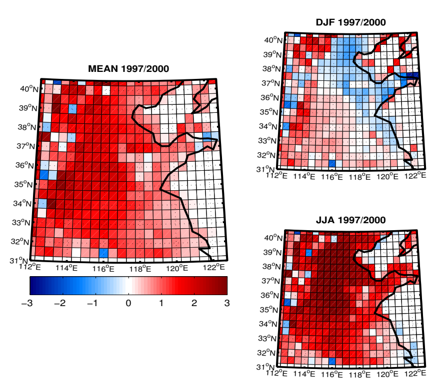

Figure 13:
Mean annual temperature: difference between the results obtained with configuration Run1 and the observed data: whole year (left panel), winter (upper right panel), summer (lower right panel)

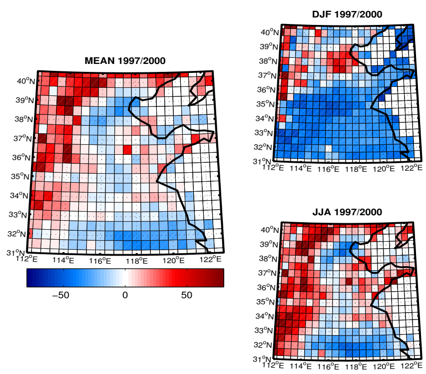

Figure 14:
Mean annual precipitation: difference between the results obtained with configuration Run1 and the observed data: whole year (left panel), winter (upper right panel), summer (lower right panel)

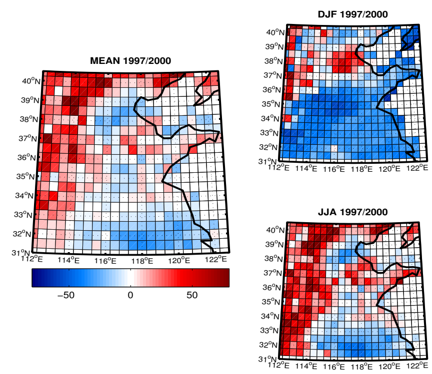

Figure 16:
Mean annual precipitation: difference between the results obtained with configuration Run2 and the observed data: whole year (left panel), winter (upper right panel), summer (lower right panel)

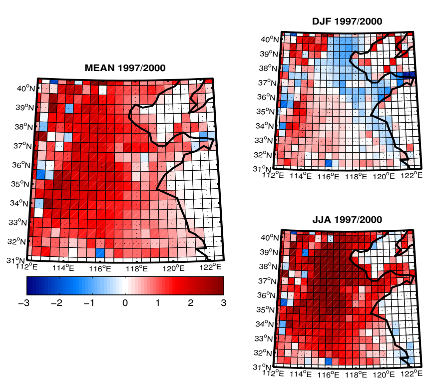

Figure 15:
Mean annual temperature: difference between the results obtained with configuration Run2 and the observed data: whole year (left panel), winter (upper right panel), summer (lower right panel)

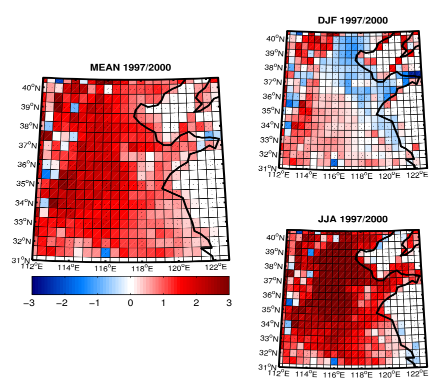

Figure 17:
Mean annual temperature: difference between the results obtained with configuration Run3 and the observed data: whole year (left panel), winter (upper right panel), summer (lower right panel)

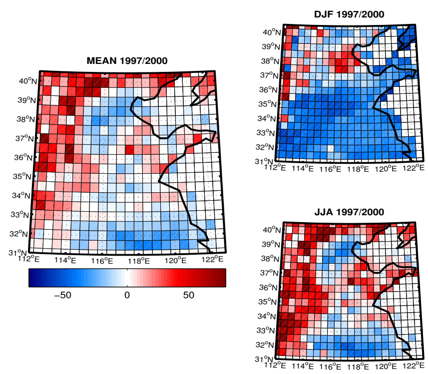

Figure 18:
Mean annual precipitation: difference between the results obtained with configuration Run3 and the observed data: whole year (left panel), winter (upper right panel), summer (lower right panel)

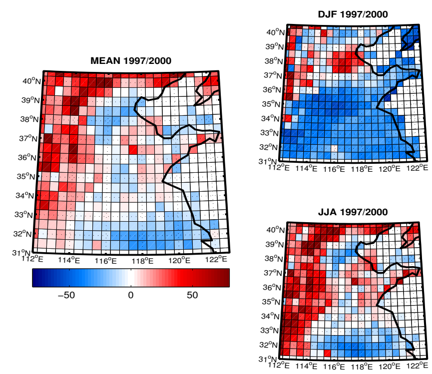

Figure 20:
Mean annual precipitation: difference between the results obtained with configuration Run4 and the observed data: whole year (left panel), winter (upper right panel), summer (lower right panel)

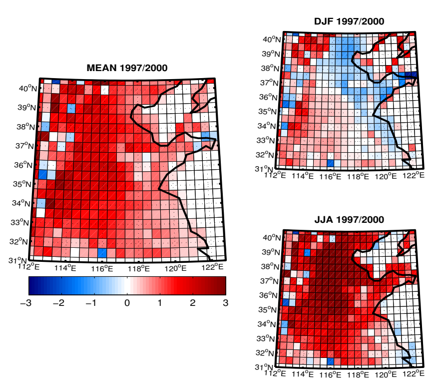

Figure 19:
Mean annual temperature: difference between the results obtained with configuration Run4 and the observed data: whole year (left panel), winter (upper right panel), summer (lower right panel)

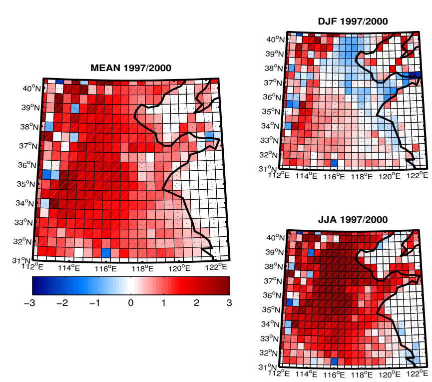

Figure 21:
Mean annual temperature: difference between the results obtained with configuration Run5 and the observed data: whole year (left panel), winter (upper right panel), summer (lower right panel)

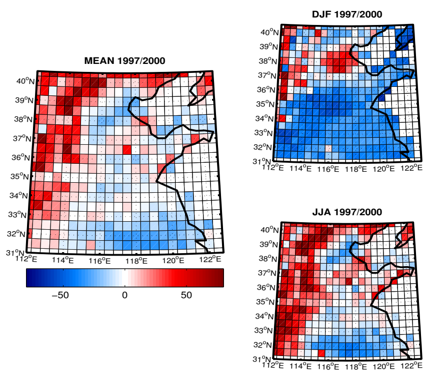

Figure 22:
Mean annual precipitation: difference between the results obtained with configuration Run5 and the observed data: whole year (left panel), winter (upper right panel), summer (lower right panel)

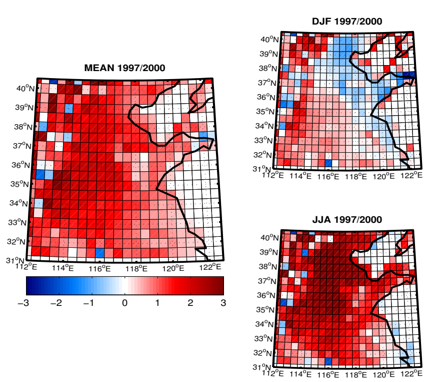

Figure 23:
Mean annual temperature: difference between the results obtained with configuration Run6 and the observed data: whole year (left panel), winter (upper right panel), summer (lower right panel)

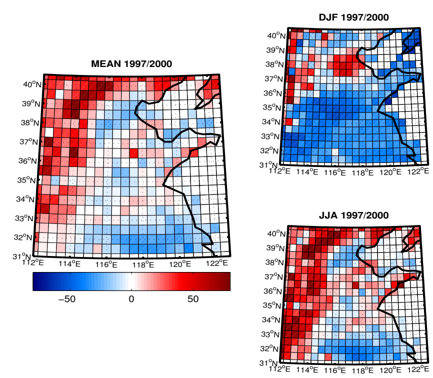

Figure 24:
Mean annual precipitation: difference between the results obtained with configuration Run6 and the observed data: whole year (left panel), winter (upper right panel), summer (lower right panel)

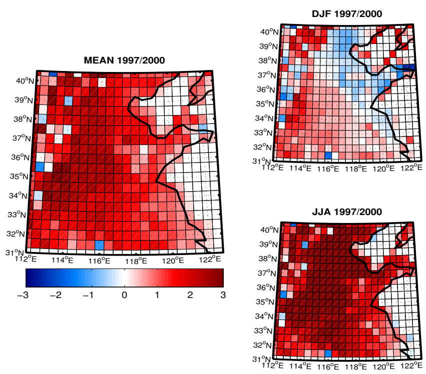

Figure 25:
Mean annual temperature: difference between the results obtained with configuration Run7 and the observed data: whole year (left panel), winter (upper right panel), summer (lower right panel)

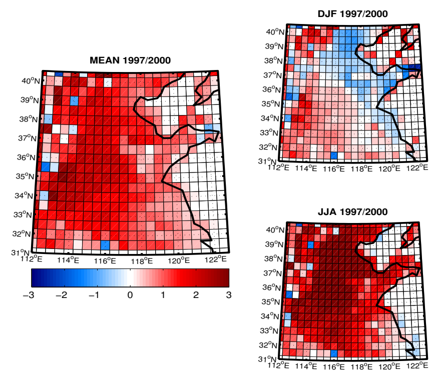

Figure 27:
Mean annual temperature: difference between the results obtained with configuration Run8 and the observed data: whole year (left panel), winter (upper right panel), summer (lower right panel)

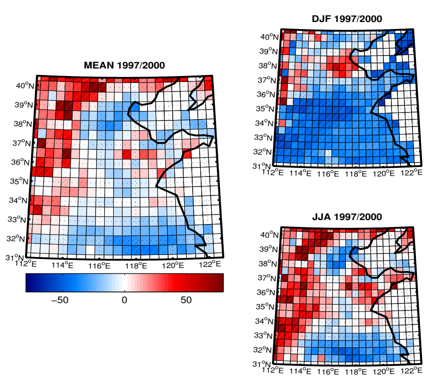

Figure 26:
Mean annual precipitation: difference between the results obtained with configuration Run7 and the observed data: whole year (left panel), winter (upper right panel), summer (lower right panel)

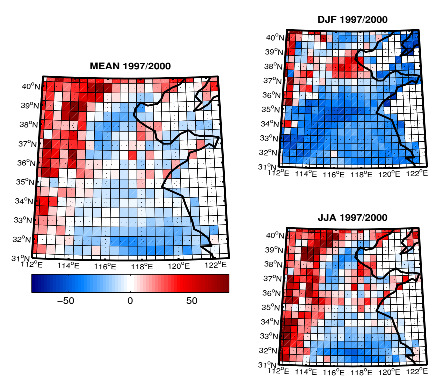

Figure 28:
Mean annual precipitation: difference between the results obtained with configuration Run8 and the observed data: whole year (left panel), winter (upper right panel), summer (lower right panel)

CONCLUSIONS

In the present work, a sensitivity analysis, incorporating eight simulations, has been performed on a test area located inside China. This work represents a necessary preliminary activity before evaluating climate scenarios for the XXI century on the Chinese region with the high resolution regional climate model COSMO CLM. The goal of this activity is the optimization of the COSMO-CLM configuration on this domain, taking into account the specific climate features of lower atmosphere temperature and precipitation. This is performed comparing the results of the different configurations with observation of 2-metre temperature and precipitation. The results show a quite good capability of the model to capture the seasonal cycle of temperature and precipitation. In fact, the temperature bias is positive and smaller than 1.4 °C for most of the simulations. Otherwise some configurations have a monthly precipitation bias (percentage) between $\pm 20\%$ with the exception of April, June and December where the bias is always higher than $\pm 20\%$ for each simulation. In conclusion, based on this preliminary activity, different configurations could be selected to perform simulation of the XXI century on the Chinese regione, namely Run1, Run4, Run5 and Run6. Therefore, to select the best configuration, the next step will be the performances evaluation of these last configurations on the whole domain (on which climate scenarios have to be simulated) for the period 1997-2000.

Bibliography

[1] U. Bohm, M. Kucken, W. Ahrens, A. Block, D. Hauffe, K. Keuler, B. Rockel, and A. Will. Clm - the climate version of lm: Brief description and long-term applications. *COSMO Newsletter*, 6:000–000, 2006.

[2] A. Dai, K.E. Trenberth, and TaoTao Q. A global dataset of Palmer Drought Severity Index for 1870-2002: Relationship with soil moisture and effects of surface warming. *Journal of Hydrometeorology*, pages 1117–1130, 2004.

[3] Y. H. Ding, Z. Y. Wang, and Y. Sun. Interdecadal variation of the summer precipitation in east china and its association with decreasing asian summer monsoon. part i: Observed evidence. *Int. J. Climatol*, 28:1139–1161, 2008.

[4] Y. H. et al. Ding. Detection, causes and projection of climate change over China: an overview of recent progress. *Adv. Atmos. Sci*, 24:954–971, 2007.

[5] J.R. Holton. *An introduction to Dynamic Meteorology*. Elsevier Academic Press, San Diego, USA, 2004.

[6] F. Lott and Miller M.J. A new subgrid-scale orographic drag parametrization: Its formulation and testing. *Q. J. R. Meteor. Soc.*, 123:101–127, 1997.

[7] G.A. Meehl, Stocker T.F., Collins W.D., P. Friedlingstein, A.T. Gaye, J.M. Gregory, A. Kitoh, R. Knutti, J.M. Murphy, S.C.B. Noda, A.and Raper, I.G. Watterson, Weaver A.J., and Zhao Z.C. *Global Climate Projections. In: Climate Change 2007: The Physical Science Basis. Contribution of Working Group I to the Fourth Assessment Report of the Intergovernmental Panel on Climate Change*. Eds: Solomon, S. and Qin, D. and Manning, M. and Chen, Z. and Marquis,M. and Averyt, K.B. and Tignor, M. and Miller H.L.. Cambridge University Press, Cambridge, United Kingdom and New York, NY, USA., 2007.

[8] T.D. Mitchell and P.D. Jones. An improved method of constructing a database of monthly climate observations and associated high resolution grids. *Int. J. Climatol.*, 25:693–712, 2005.

[9] S. Piao, P. Ciais, Y. Huang, Z. Shen, S. Peng, J. Li, L. Zhou, H. Liu, Y. Ma, Y. Ding, P. Friedlingstein, C. Liu, K. Tan, Y. Yu, T. Zhang, and J. Fang. The impacts of climate change on water resources and agriculture in China. *Nature*, 467(7311):43–51, September 2010.

[10] B. Rockel and B. Geyer. The performance of the regional climate model CLM in different climate regions, based on the example of precipitation. *Meteorologische Zeitschrift*, 17(4):487–498, August 2008.

[11] B. Rockel, A. Will, and A. Hense. The regional climate model cosmo-clm (cclm). *Meteorologische Zeitschrift*, 17(4):347–348, 2008.

[12] C. Schar, D. Leuenberger, O. Fuhrer, D. Luthi, and C. Girard. A new terrain-following vertical coordinate formulation for atmospheric prediction models. *Mon. Wea. Rev.*, 130:2459–2480, 2002.

[13] J. Steppeler, G. Doms, U. Schï¿½ttler, H.W. Bitzer, A. Gassmann, U. Damrath, and Gregoric G. Meso-gamma scale forecasts using the non-hydrostatic model lm. *Meteorol. Atmos. Phys.*, 82:75–96, 2003.

[14] S.M. Uppala. The era-40 re-analysis. *Quart. J. Roy. Meteor. Soc.*, 612:2961–3012, 2006.

[15] K. Wei and W. Chen. Climatology and trends of high temperature extremes across China in summer. *Atmos. Ocean. Sci. Lett*, 2:153–158, 2009.

[16] Q. You. Changes in daily climate extremes in china and their connection to the large scale atmospheric circulation during 1961-2003. *Climate Dynamics*, DOI 10.1007/s00382-009-0735-0:000–000, 2009.